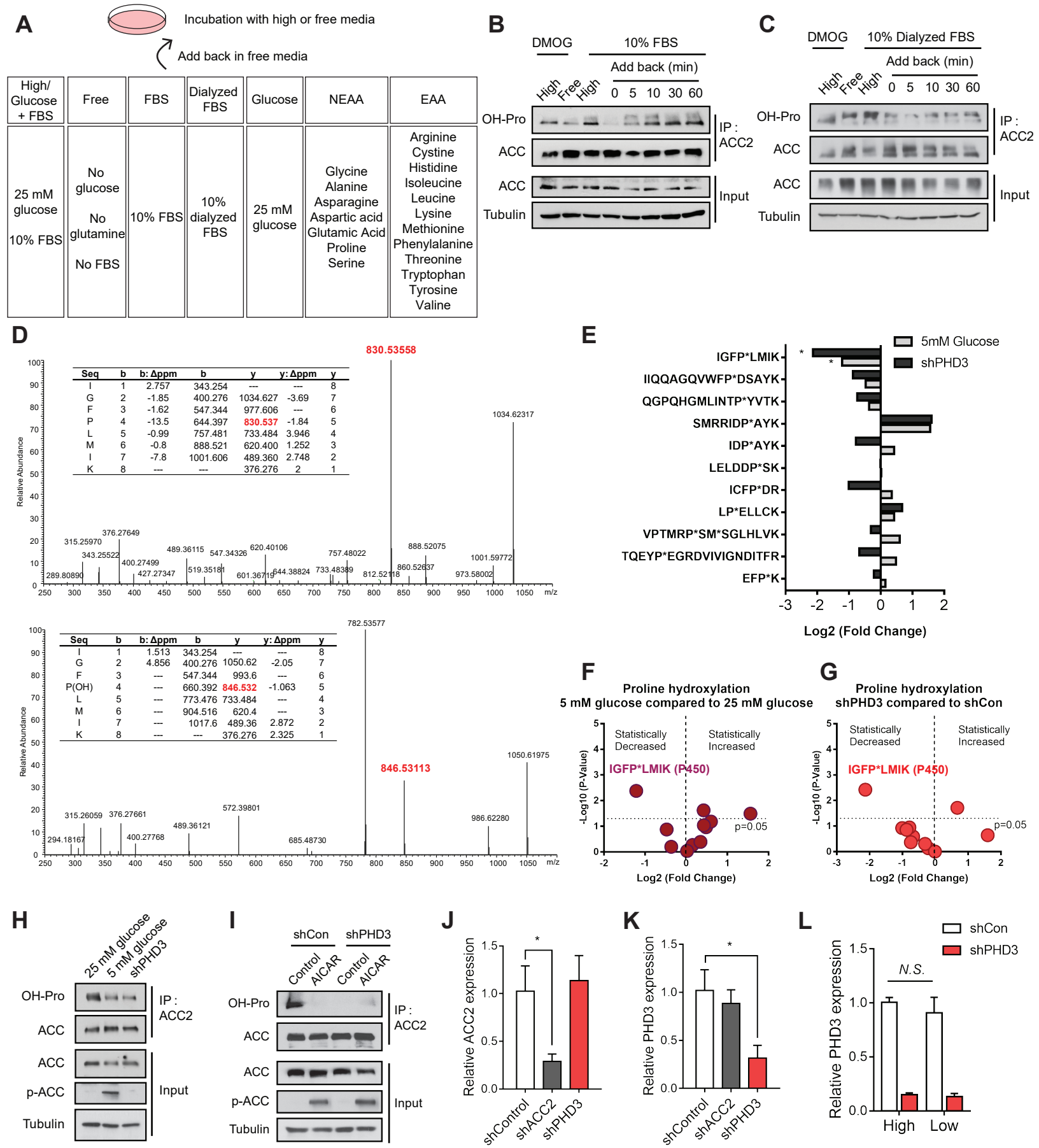
A
Incubation with high or free media
Add back in free media
High/ Glucose + FBS
Free
FBS
Dialyzed FBS
Glucose
NEAA
EAA
25 mM glucose
10% FBS
No glucose
No glutamine
No FBS
10% FBS
10% dialyzed FBS
25 mM glucose
Glycine
Alanine
Asparagine
Aspartic acid
Glutamic Acid
Proline
Serine
Arginine
Cystine
Histidine
Isoleucine
Leucine
Lysine
Methionine
Phenylalanine
Threonine
Tryptophan
Tyrosine
Valine
B
DMOG
10% FBS
Add back (min)
High
Free
High
0 5 10 30 60
OH-Pro
ACC
ACC
Tubulin
IP : ACC2
Input
C
DMOG
10% Dialyzed FBS
Add back (min)
High
Free
High
0 5 10 30 60
OH-Pro
ACC
ACC
Tubulin
IP : ACC2
Input
D
830.53558
Seq b b: Δppm b y y: Δppm y
I 1 2.757 343.254 --- --- 8
G 2 -1.85 400.276 1034.627 -3.69 7
F 3 -1.62 547.344 977.606 --- 6
P 4 -13.5 644.397 830.537 -1.84 5
L 5 -0.99 757.481 733.484 3.946 4
M 6 -0.8 888.521 620.400 1.252 3
I 7 -7.8 1001.606 489.360 2.748 2
K 8 --- --- 376.276 2 1
1034.62317
376.27649
315.25970
343.25522
400.27499
427.27347
489.36115
519.35181
547.34326
620.40106
644.38824
757.48022
733.48389
812.52118
860.52637
888.52075
973.58002
1001.59772
289.80890
601.36719
Relative Abundance
m/z
782.53577
Seq b b: Δppm b y y: Δppm y
I 1 1.513 343.254 --- --- 8
G 2 4.856 400.276 1050.62 -2.05 7
F 3 --- 547.344 993.6 --- 6
P(OH) 4 --- 660.392 846.532 -1.063 5
L 5 --- 773.476 733.484 --- 4
M 6 --- 904.516 620.4 --- 3
I 7 --- 1017.6 489.36 2.872 2
K 8 --- --- 376.276 2.325 1
846.53113
1050.61975
315.26059
376.27661
400.27768
489.36121
572.39801
685.48730
986.62280
294.18167
Relative Abundance
m/z
E
5mM Glucose
shPHD3
IGFP*LMIK
IIQQAGQVWFP*DSAYK
QGPQHGMLINTP*YVTK
SMRRIDP*AYK
IDP*AYK
LELDDP*SK
ICFP*DR
LP*ELLCK
VPTMRP*SM*SGLHLVK
TQEYP*EGRDVIVIGNDITFR
EFP*K
Log2 (Fold Change)
F
Proline hydroxylation
5 mM glucose compared to 25 mM glucose
Statistically Decreased
Statistically Increased
IGFP*LMIK (P450)
p=0.05
-Log10 (P-Value)
Log2 (Fold Change)
G
Proline hydroxylation
shPHD3 compared to shCon
Statistically Decreased
Statistically Increased
IGFP*LMIK (P450)
p=0.05
-Log10 (P-Value)
Log2 (Fold Change)
H
25 mM glucose
5 mM glucose
shPHD3
OH-Pro
ACC
ACC
p-ACC
Tubulin
IP : ACC2
Input
I
shCon
shPHD3
Control
AICAR
Control
AICAR
OH-Pro
ACC
ACC
p-ACC
Tubulin
IP : ACC2
Input
J
Relative ACC2 expression
shControl
shACC2
shPHD3
K
Relative PHD3 expression
shControl
shACC2
shPHD3
L
shCon
shPHD3
N.S.
Relative PHD3 expression
High
Low

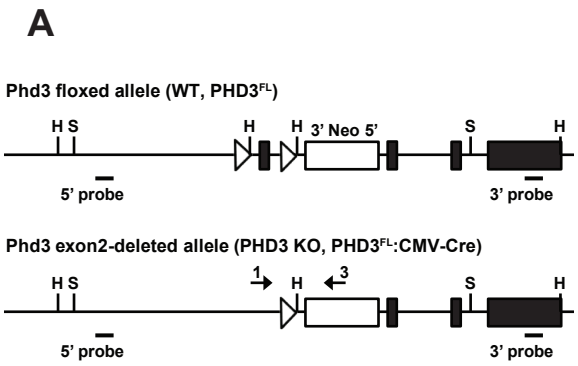
A
Phd3 floxed allele (WT, PHD3FL)
H S
H
H
3' Neo 5'
S
H
5' probe
3' probe
Phd3 exon2-deleted allele (PHD3 KO, PHD3FL:CMV-Cre)
1
3
H S
H
S
H
5' probe
3' probe

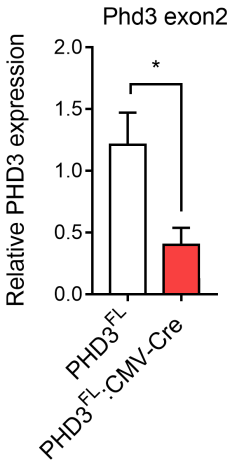
B
Phd3 exon2
Relative PHD3 expression
2.0
1.5
1.0
0.5
0.0
*
PHD3FL
PHD3FL:CMV-Cre

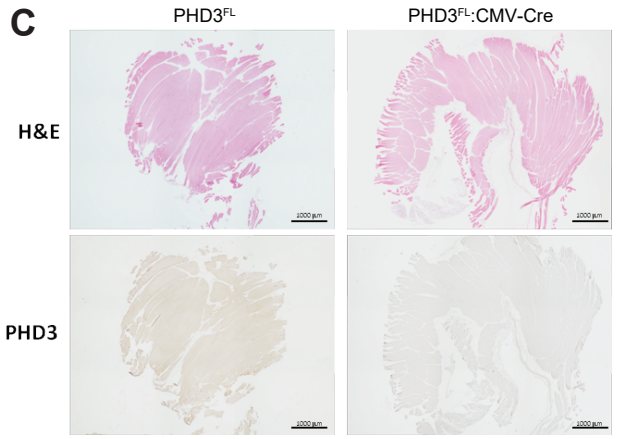
C
PHD3FL
PHD3FL:CMV-Cre
H&E
PHD3

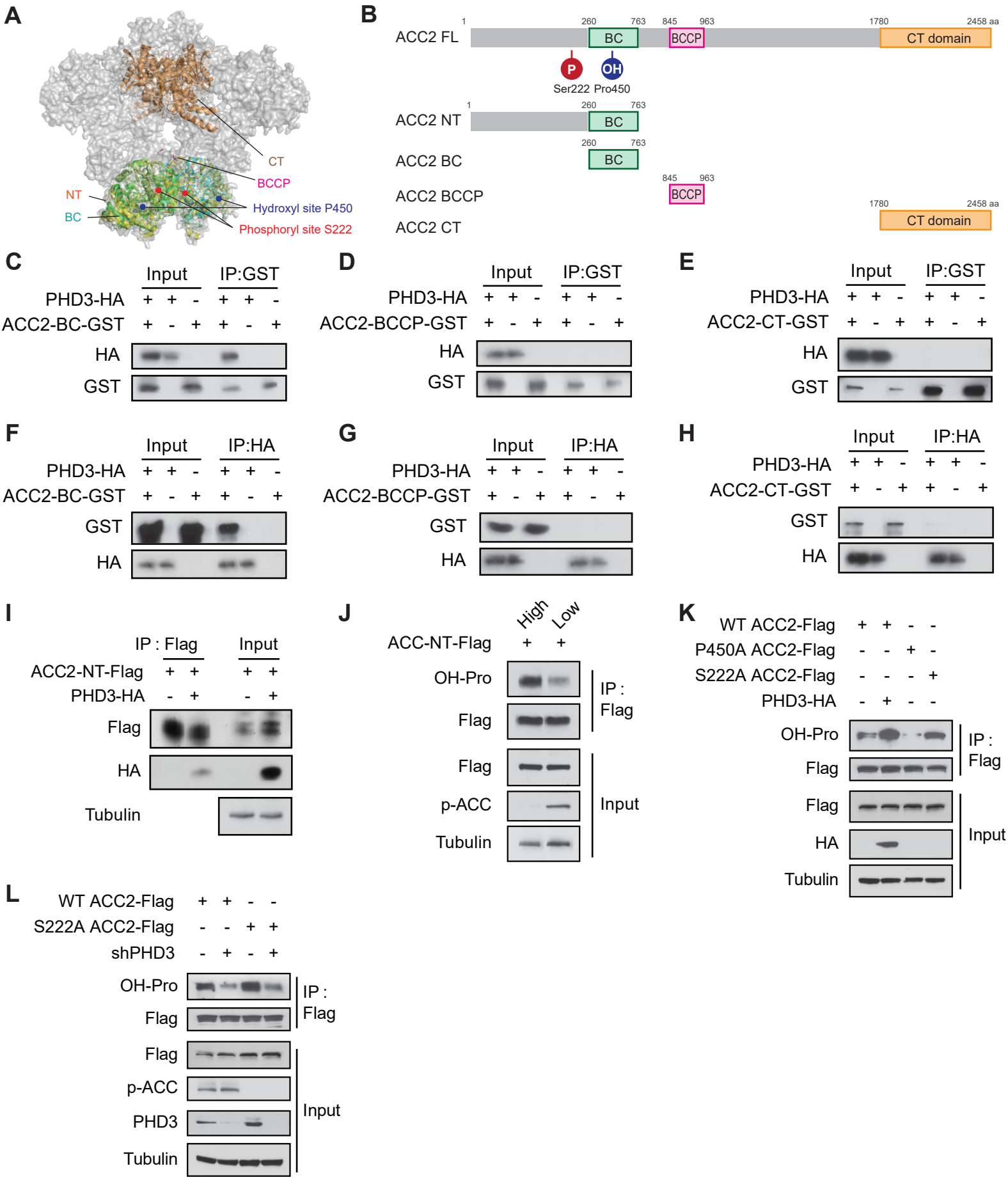
A
CT
BCCP
NT
BC
Hydroxyl site P450
Phosphoryl site S222
B
ACC2 FL
1
260
763
845
963
1780
2458 aa
BC
BCCP
CT domain
P
OH
Ser222 Pro450
ACC2 NT
ACC2 BC
ACC2 BCCP
ACC2 CT
C
Input
IP:GST
PHD3-HA
ACC2-BC-GST
HA
GST
D
ACC2-BCCP-GST
E
ACC2-CT-GST
F
IP:HA
G
H
I
IP : Flag
ACC2-NT-Flag
Flag
Tubulin
J
High
Low
OH-Pro
p-ACC
K
WT ACC2-Flag
P450A ACC2-Flag
S222A ACC2-Flag
L
shPHD3
PHD3

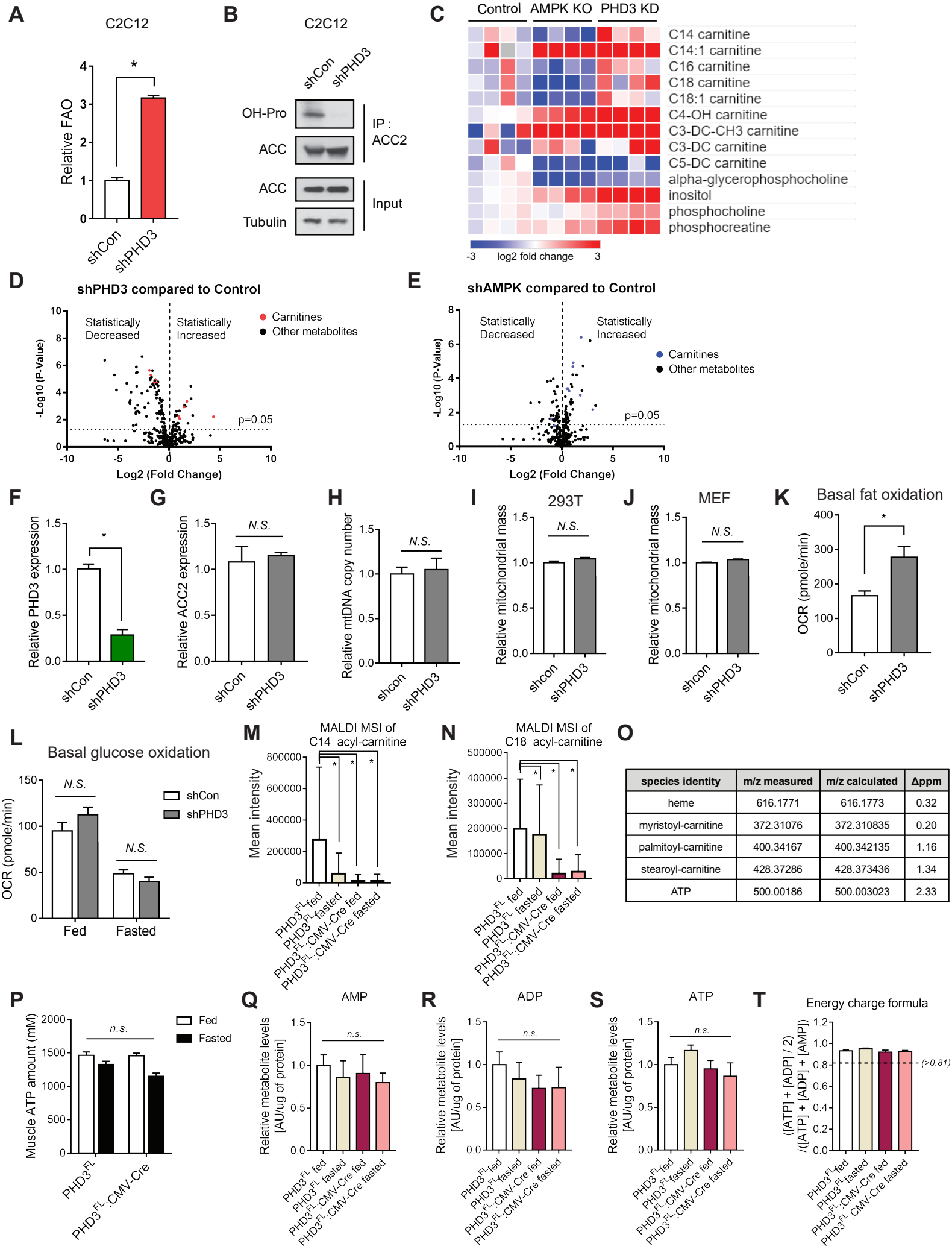

species identity	m/z measured	m/z calculated	Δppm
heme	616.1771	616.1773	0.32
myristoyl-carnitine	372.31076	372.310835	0.20
palmitoyl-carnitine	400.34167	400.342135	1.16
stearoyl-carnitine	428.37286	428.373436	1.34
ATP	500.00186	500.003023	2.33

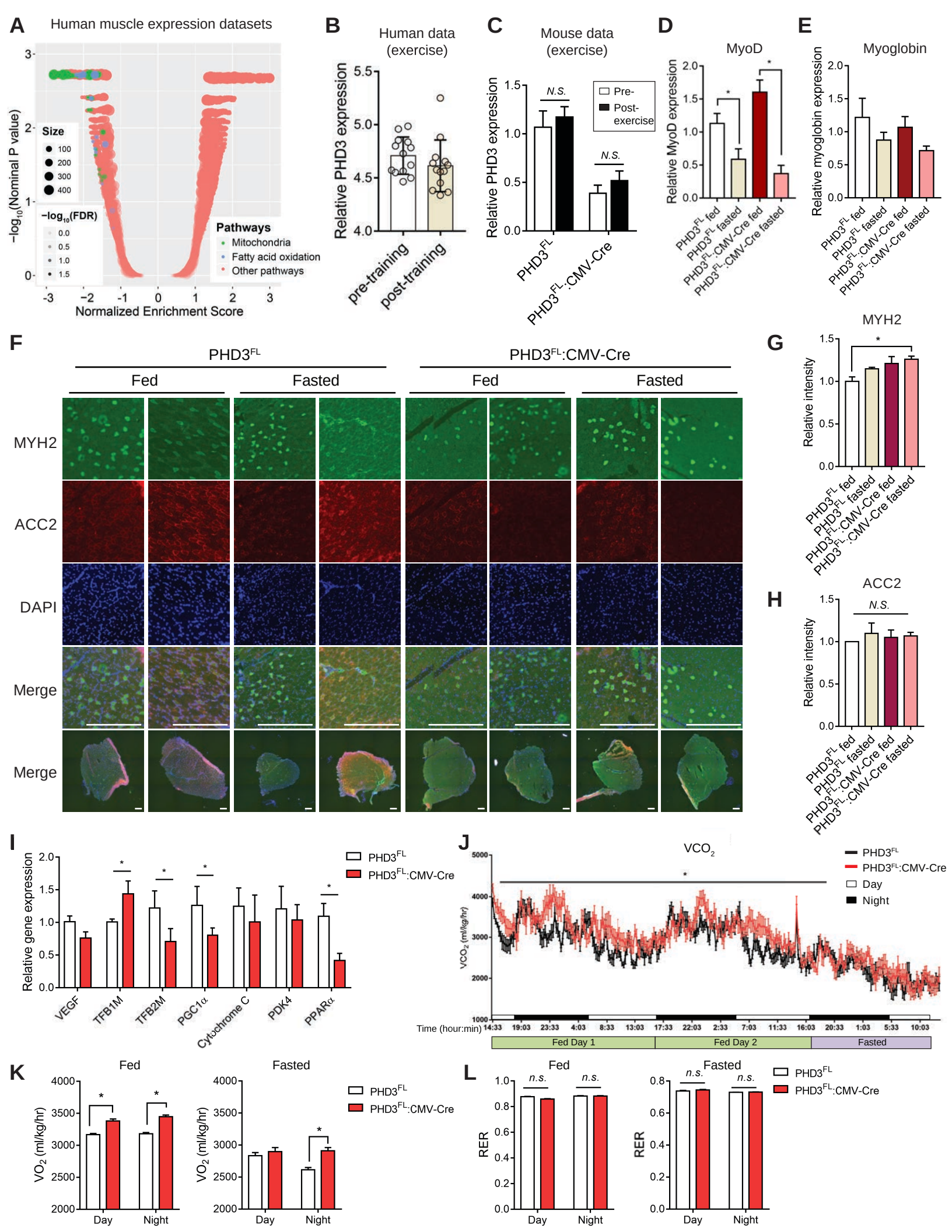
A
Human muscle expression datasets
−log10(Nominal P value)
Size
100
200
300
400
−log10(FDR)
0.0
0.5
1.0
1.5
Pathways
Mitochondria
Fatty acid oxidation
Other pathways
Normalized Enrichment Score
B
Human data (exercise)
Relative PHD3 expression
pre-training
post-training
C
Mouse data (exercise)
Relative PHD3 expression
N.S.
Pre-exercise
Post-exercise
PHD3FL
PHD3FL:CMV-Cre
D
MyoD
Relative MyoD expression
PHD3FL fed
PHD3FL fasted
PHD3FL:CMV-Cre fed
PHD3FL:CMV-Cre fasted
E
Myoglobin
Relative myoglobin expression
F
PHD3FL
PHD3FL:CMV-Cre
Fed
Fasted
MYH2
ACC2
DAPI
Merge
Merge
G
MYH2
Relative intensity
H
ACC2
N.S.
Relative intensity
I
Relative gene expression
VEGF
TFB1M
TFB2M
PGC1α
Cytochrome C
PDK4
PPARα
J
VCO2
Time (hour:min)
Day
Night
Fed Day 1
Fed Day 2
Fasted
K
Fed
Fasted
VO2 (ml/kg/hr)
Day
Night
L
Fed
Fasted
RER
n.s.

A

PHD3^{FL} or PHD3^{FL}:CMV-Cre

Time (min)	0	5	10	15	20	25	30	35	40	45	50	55	60	65	70
Speed (m/min)	0	0	0	0	5	10	15	20	20	20	20	20	20	20	20
Incline	0	0	0	0	0	0	0	0	5	10	15	20	25	25	25

B

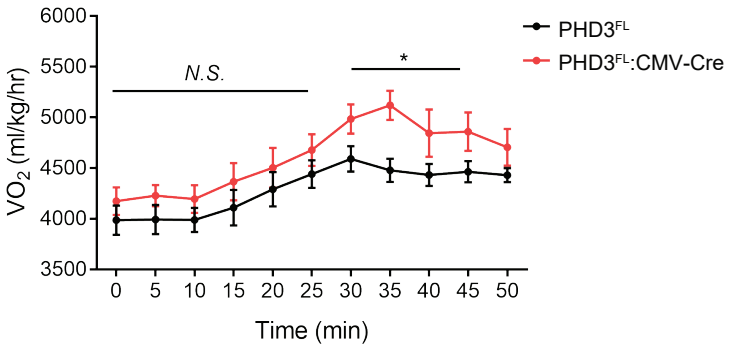

C

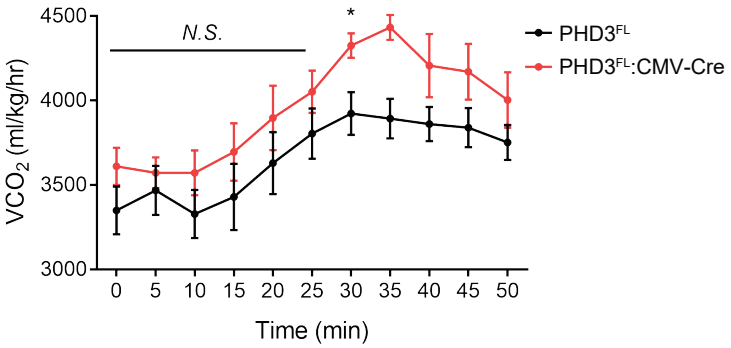

D

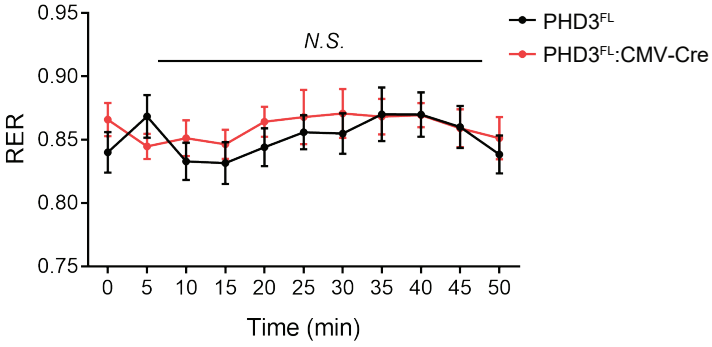

E

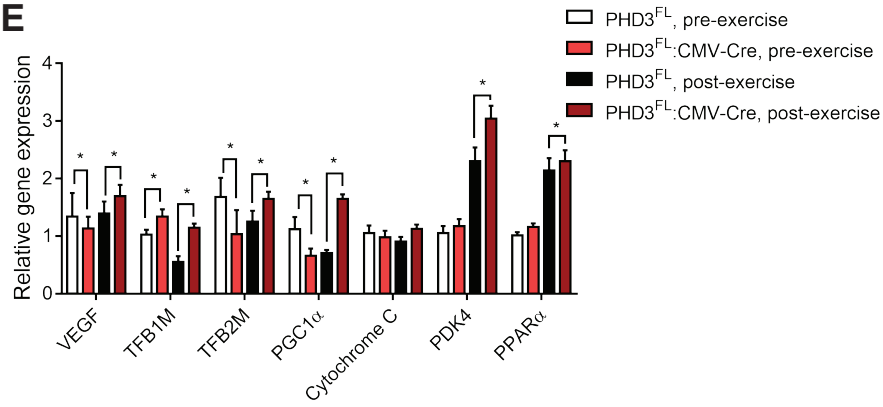

F

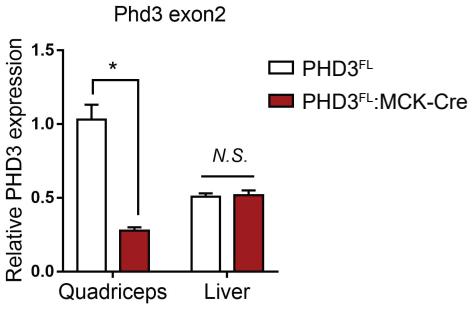

G

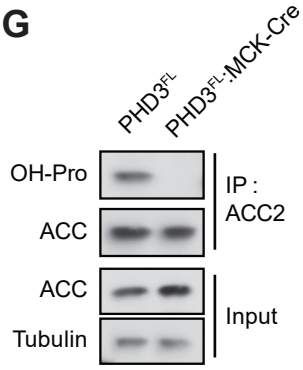

Supplement Table 1. primer sequences, Related to Figure2, Figure 5 and Figure 6.

RT-PCR Primers	
Name	**Sequence**
human PHD3 Forward	ATACTACGTCAAGGAGAGGT
human PHD3 Reverse	TCAGCATCAAAGTACCAGA
human B2M Forward	AGATGAGTATGCCTGCCGTGTGAA
human B2M Reverse	TGCTGCTTACATGTCTCGATCCCA
human ACC2 Forward	CTCTGACCATGTTCGTTCTC
human ACC2 Reverse	ATCTTCATCACCTCCATCTC
mouse PHD3 Forward	CAGACCGCAGGAATCCACAT
mouse PHD3 Reverse	TTCAGCATCGAAGTACCAGACAGT
mouse ACC2 Forward	TTCATGGACAGTGGCTTCTC
mouse ACC2 Reverse	GCACGCCTTACTGAAGAGAAG
mouse VEGF Forward	AAAAACGAAAGCGCAAGAAA
mouse VEGF Reverse	TTTCTCCGCTCTGAACAAGG
mouse TFB1 Forward	AATTTCCTCCTGGACTTGAGG
mouse TFB1 Reverse	AGAGAGCATCTGTAACCCTGG
mouse TFB2 Forward	GTTCGAATGACTCCTCGTAGG
mouse TFB2 Reverse	CATTCTAGCAGCTGTGTCTCC
mouse PGC-1α Forward	CCCTGCCATTGTTAAGACC
mouse PGC-1α Reverse	TGCTGCTGTTCCTGTTTTC
mouse Cytochrome C Forward	CACGCTTTACCCTTCGTTCT
mouse Cytochrome C Reverse	CTCATTTCCCTGCCATTCTCTA
mouse PDK4 Forward	CCGCTGTCCATGAAGCA
mouse PDK4 Reverse	GCAGAAAAGCAAAGGACGTT
mouse PPARα Forward	AGAGCCCCATCTGTCCTCTC
mouse PPARα Reverse	ACTGGTAGTCTGCAAAACCAAA
mouse β-Actin Forward	AGCCATGTACGTAGCCATCC
mouse β-Actin Reverse	CTCTCAGCTGTGGTGGTGAA

Primers for MT-DNA Copy Number	
Name	**Sequence**
MT-CO2 Forward	CCCCACATTAGGCTTAAAAACAGAT
MT-CO2 Reverse	TATACCCCCGGTCGTGTAGCGGT
D-Loop Forward	TATCTTTTGGCGGTATGCACTTTTAACAG
D-Loop Reverse	TGATGAGATTAGTAGTATGGGAGTGG
β-Globin Forward	GTGCACCTGACTCCTGAGGAGA
β-Globin Reverse	CCTTGATACCAACCTGCCCAG
β-Actin Forward	TCACCCACACTGTGCCCATCTACGA
β-Actin Reverse	CAGCGGAACCGCTCATTGCCAATGG

Primers for cloning	
Name	**Sequence**
ACC2 P450A Forward	AATTGGTTTTgcaTTGATGATCAAAG
ACC2 P450A Reverse	CTTTCTGCTGCCTCCAAG
ACC2 S222A Forward	GCCGAGCATGgcgGGACTCCACC
ACC2 S222A Reverse	CTCATAGTGGGGACGCGGGTC
ACC2 S222E Forward	GCCGAGCATGgagGGACTCCACC
ACC2 S222E Reverse	CTCATAGTGGGGACGCGGGTC
ACC2 BC Forward	CTGGGATCCCCGGAATTCGATGATCTGCAGCAGGGAAAA
ACC2 BC Reverse	CGTCAGTCAGTCACGATGCATGGCGATCTGTAGCTGG
ACC2 BCCP Forward	CTGGGATCCCCGGAATTCACAGTCCTGAGATCCCCC
ACC2 BCCP Reverse	CGTCAGTCAGTCACGATGCAGCCTGGCCACCAC
ACC2 CT Forward	CTGGGATCCCCGGAATTCCTTCTGTACCTGCGGGCA
ACC2 CT Reverse	CGTCAGTCAGTCACGATGGCCGGGTGTGTCATGGAA
ACC2 NT Forward	CCGGAATTCAAGGGCAGCCGGGCCAGCTTG
ACC2 NT Reverse	CGTCAGTCAGTCACGATGCATGGCGATCTGTAGCTGG

Primers for shRNA knockdowns	
Name	**Sequence**
Control shRNA Forward	CCGGCCGTCATAGCGATAACGAGTTCTCGAGAACTCGTTATCGCTATGACGGTTTTTG
Control shRNA Reverse	AATTCAAAAACCGTCATAGCGATAACGAGTTCTCGAGAACTCGTTATCGCTATGACGG
shPHD3 #1 (TRCN0000001048)	CACCTGCATCTACTATCTGAA
shPHD3.2 (TRCN0000001050)	GTGGCTTGCTATCCGGGAAAT
shACC2 #1 (TRCN 0000029031)	CCGACGAATCACATTCTTGAT
shACC2 #2 (TRCN 0000029032)	CCCGAGAACCTCAAGAAATTA

SUPPLEMENTARY FIGURE LEGENDS

Figure S1.Nutrient and PHD3-dependent changes in ACC2 proline hydroxylation. Related to Figure 1.

(A) Schematic depicting different fuels examined in nutrient add back assays. After fuel addition, cells were used for ACC2 hydroxylation assay. MEF cells were cultured in high or low glucose for 12 h, then hydroxylation was assessed at the indicated times after re-addition of 10% FBS (B), or 10% dialyzed FBS (C). Proline hydroxylation was detected in ACC2 immunoprecipitates by western blotting using antibodies to pan-proline hydroxylation, compared with ACC or tubulin controls from the input cell lysate. (D) Representative mass spectra identifying the hydroxylated and non-hydroxylated versions of residue P450 in immunoprecipitated ACC2 protein. ‘‘b’’ fragments contain the N-terminal amino acid and are labeled from the N to C terminus. ‘‘y’’ fragments contain the C-terminal amino acid and are labeled from the C to N terminus. (E) Relative abundance of hydroxylation of proline residues on ACC2 immunoprecipitated from MEFs cultured in 5 mM versus 25 mM glucose media (light grey) or control vs. shPHD3 knockdown cells (dark grey). For all comparisons two-tailed t test was used. $P < 0.05$. (F-G) Volcano plots demonstrating that 5 mM glucose media (F) or PHD3-depleted MEFs (G) incubated MEFs have statistically significant proline hydroxylation changes compared to control cells. The proline 450 residue, (aa sequence: IGFP(OH)LMIK), was most significantly changed. (H) Immunoprecipitation and western blotting analysis of ACC2 hydroxylation and phosphorylation in the indicated condition. shControl or shPHD3 293T cells were transfected with ACC2, and incubated with 25 mM glucose media or 5 mM glucose media for 4 h. ACC2 proteins were pulled down using antibody against ACC2 and immunoblotted using the indicated antibodies. (I) Immunoblots of ACC2 hydroxylation from MEFs expressing either control shRNA or PHD3 shRNA with or without AICAR. (J) Relative ACC2 expression using mouse β-actin as a reference gene in MEFs expressing shRNA against ACC2, PHD3 or shRNA control ($n = 4$). (K) Relative PHD3 expression using mouse β-actin as a reference gene in MEFs expressing shRNA against ACC2, PHD3 or shRNA control ($n = 4$). (L) PHD3 expression using mouse b-actin as a reference gene in MEFs under high or low nutrient conditions.

Figure S2. PHD3 KO mouse generation. Related to Figure 2.

(A) Gene targeting strategy for Phd3. In the Phd3 locus, exon 2 is flanked by two loxP sites. Exon 2 is deleted by Cre-mediated recombination. S, Sca I; H, Hind III; Neo, neomycin cassette; hatched square, Frt site (flanking the Neo cassette); open triangle, loxP site; arrows 1, 2 and 3. (B) qPCR analyses to confirm the lack of WT mRNA transcripts in PHD3 KO mouse quadriceps. (C) H&E and immunohistochemistry staining of PHD3 in WT or PHD3 KO mice quadriceps muscles. Scale is 1000 μm.

Figure S3. PHD3 binds the BC domain of ACC2. Related to Figure 3.

(A) P450 (hydroxylation site, blue) is located in the ACC2 BC domain (green and cyan). S222 (phosphorylation site, red) is located inside of the ACC holoenzyme dimer structure. This model

was generated by superposition of human ACC2 biotin carboxylase domain (PDB: 3JRW) with the entire yeast ACC (PDB: 5CSL). (B) Schematic figure of the domains of ACC2 protein. Posttranslational modifications by AMPK (phosphorylation, red) and PHD3 (hydroxylation, blue) are highlighted. BC, biotin carboxylase domain; BCCP, biotin carboxyl carrier protein domain; CT, carboxyltransferase domain; N-terminus domain contains ATP grasp domain. (C) Immunoprecipitation and western blotting analysis of PHD3 interaction with the BC domain of ACC2. Proteins were expressed in *e. coli*. ACC2 BC domain with GST-tag and PHD3-HA was pulled down using GST-beads for an *in vitro* binding assay, and the precipitates were immunoblotted. (D) *In vitro* binding of PHD3 with the BCCP domain of ACC2 was assessed by immunoprecipitating protein complexes using anti-GST-beads. (E) *In vitro* binding assay of PHD3 interaction with the CT domain using anti-GST-beads. (F) Immunoprecipitation using anti-HA-beads and western blotting analysis of PHD3 interaction with the BC domain of ACC2. *In vitro* binding assay of PHD3 interaction with the BCCP domain (G) or CT domain (H). (I) HEK293T cells were transfected with constructs expressing ACC2 NT-Flag and/or PHD3-HA. Proteins from cell lysates were immunoprecipitated using anti-Flag antibody and the immunoprecipitates were immunoblotted using the indicated antibodies. (J) ACC2 NT-Flag was transfected into HEK293T cells. Cells were incubated in high (25 mM) or low (5 mM) glucose containing media for 8 hr. Proteins in cell lysates were precipitated by anti-Flag antibody and the precipitates were immunoblotted using hydroxyl proline antibodies. (K) ACC2 FL-WT-Flag, ACC2 FL-P450A-Flag, ACC2 FL-S222A-Flag and/or PHD3-HA were transfected into MEFs. Complexes were immunoprecipitated using anti-Flag antibody and proteins were detected by immunoblotting using the indicated antibodies. (L) Immunoprecipitation and western blot analysis in shcontrol or shPHD3 MEFs overexpressing full length WT ACC2 or S222A ACC2. (M-P) *In vitro* hydroxylation assay for PHD3 enzymatic activity with recombinant protein about N-terminus domains of WT ACC2 (M), P450A ACC2 (N), S222A (O), or S222E (P). 2.5 uM or 5 uM of PHD3 WT, or H196A mutants were added to a reaction with 20 uM synthetic peptide and then succinate was measured at the indicated times. Rates were normalized against the No peptide control (n=3). *$P < 0.05$.

Figure S4. PHD3 regulation of fat metabolism. Related to Figure 4

(A) Palmitate oxidation in shCon (control) or shPHD3 C2C12 cells using ^{3}H-palmitate as a substrate and measuring released $^{3}H_2O$ as readout for FAO (n=3). (B) Proline hydroxylation was assessed by immunoblotting from anti-ACC2 immunoprecipates and corresponding whole-cell lysates of shcontrol or shPHD3 C2C12 cells. (C) Heat map depicting metabolite abundance in PHD3 knockdown, AMPKα knockout or non-silencing control MEFs. Volcano plots demonstrating that PHD3 (D) and AMPK depleted MEFs (E) have numerous statistically significant metabolic changes compared to control cells. PHD3 expression (F) or ACC2 expression (G) using B2M as a reference gene in shControl or shPHD3 HEK293T cells. (H) Mitochondrial DNA number was not changed by PHD3 knockdown. mtDNA levels were measured by quantitative PCR of MT-CO_2 using human b-actin as a reference gene in shControl or shPHD3 HEK293T cells. Mitochondrial mass of 293T cells (I) or MEFs (J) depleted of PHD3 or control shRNA using MitoTracker Green (n = 5). (K) Basal palmitate-driven oxygen consumption rate (OCR) of shControl or shPHD3 MEFs was measured using a Seahorse Bioscience XF24 Extracellular Flux Analyzer (n = 15 wells). (L) Basal oxygen consumption rate

(OCR) of shControl or shPHD3 MEFs cultured in high or low glucose media was measured using a Seahorse Bioscience XF24 Extracellular Flux Analyzer (n = 15 wells). Matrix-assisted laser desorption/ionization mass spectrometry imaging (MALDI-MSI) of myristoyl-carnitine (m/z 372.310835, Δppm = 0.2) (M), and stearoyl-carnitine (m/z 428.37286, Δppm = 1.34) (N) in WT or PHD3 KO mouse quadriceps under fed or fasted conditions. (O) Measured and calculated mass of species detected by MALDI MS (FT-ICR MS so <2 ppm expected). (P) ATP levels were measured in quadriceps tissue lysates in WT or PHD3 KO mice under fed or fasted condition (n=4) using ATP colorimetric assay kit. ATP, ADP and AMP were measured in WT or PHD3 KO mice quadriceps tissues using mass spectrometry. ATP (Q), ADP (R) and AMP (S) levels were measured in fresh frozen quadriceps tissue in the indicated conditions. WT or PHD3 KO mice under fed or fasted condition (n=8). (T) The energy charge formula was calculated through ([ATP] + [ADP] / 2) / ([ATP] + [ADP] + [AMP]).

Figure S5. PHD3 KO mouse muscle characterization. Related to Figure 5

(A) Gene set enrichment analysis of PHD3 indicating its negative connection with fatty acid oxidation and mitochondrial pathways in human muscle dataset (GSE3307). Mitochondrial and fatty acid oxidation pathways are highlighted in green and blue, respectively. The size of dot represents the number of genes in the pathway, and transparency indicates the significance (-log10 (FDR)) of the enrichment between this pathway and PHD3 expression. (B) PHD3 expression levels in human muscle biopsies in pre-exercise or post-exercise training (GSE111551). Data represent means ± SEM. (C) Relative PHD3 expression using mouse beta-actin as a reference gene in WT or PHD3 KO mice quadriceps pre-exercise versus post exercise (n=9). The mRNA levels of MyoD (D) and myoglobin (E) in WT or PHD3 KO mouse quadriceps under fed or fasting conditions (n = 4). *P < 0.05. (F) Immunofluorescence of Myosin Heavy Chain Type IIA (MYH2) (green), ACC2 (red) and DAPI (blue) in Flox (WT) or PHD3 KO mouse quadriceps under fed and fasted conditions. Scale is 500 μm. (G-H) The relative intensity of MYH2 (G) and ACC2 (H) were normalized by the relative intensity of DAPI for each condition. (I) Gene expression using mouse β-actin as a reference gene in WT or PHD3 KO mouse quadriceps (n = 4). (J) Mean whole-body CO_2 analysis in 20 week-old WT or PHD3 KO mice using Comprehensive Lab Animal Monitoring System (CLAMS) (n=9). WT or PHD3 KO mice were subjected to ad libitum feeling for 48 hours, followed by fasting for 16 hours. Mean whole-body oxygen consumption (K) and Respiratory exchange ratio (RER) (L) in WT or PHD3 KO mice under fed and fasted conditions using CLAMS. Data represented means ± SEM. *P < 0.05.

Figure S6. PHD3 KO mice have increased exercise capacity compared to WT littermates. Related to Figure 6.

(A) Schematic of the exercise capacity treadmill experiment. (B) Age-matched mice (20 weeks old) were individually placed in metabolic cages and allowed to acclimate for 48 h before experiments (n = 8 mice per group). Mean whole-body oxygen consumption of both genotypes from the individual performances. (C) Mean whole-body CO_2 during exercise challenge, beginning with mice at rest. (D) RER (VCO_2/VO_2). Data represented means ± SEM. *P < 0.05.

(E) Expression of the indicated genes from WT or PHD KO mouse quadriceps pre- or immediately post-exercise. Mouse β-actin was used as a reference gene (n=4). (F) qPCR analyses of WT PHD3 mRNA transcript in WT or PHD3 MCK-Cre KO mouse quadriceps and liver RNA samples. (G) ACC2 immunoprecipitation and western blotting analysis of ACC2 hydroxylation in WT control or PHD3 MCK-Cre KO mice quadriceps.